J|A|C|S
ARTICLES

Published on Web 06/06/2008

Role of Exposed Metal Sites in Hydrogen Storage in MOFs

Jenny G. Vitillo,[†] Laura Regli,[†] Sachin Chavan,[†] Gabriele Ricchiardi,[†] Giuseppe Spoto,[†] Pascal D. C. Dietzel,[‡] Silvia Bordiga,*[,†] and Adriano Zecchina[†]

Dipartimento di Chimica IFM and NIS Centre of Excellence, Università di Torino, Via Pietro Giuria 7, 10125 Torino and INSTM UdR Torino, Italy and SINTEF Materials and Chemistry, Department of Hydrocarbon Process Chemistry, P.O. Box 124 Blindern, 0314 Oslo, Norway

Received February 5, 2008; E-mail: silvia.bordiga@unito.it

Abstract: The role of exposed metal sites in increasing the H_2 storage performances in metal−organic frameworks (MOFs) has been investigated by means of IR spectrometry. Three MOFs have been considered: MOF-5, with unexposed metal sites, and HKUST-1 and CPO-27-Ni, with exposed Cu^{2+} and Ni^{2+}, respectively. The onset temperature of spectroscopic features associated with adsorbed H_2 correlates with the adsorption enthalpy obtained by the VTIR method and with the shift experienced by the H−H stretching frequency. This relationship can be ascribed to the different nature and accessibility of the metal sites. On the basis of a pure energetic evaluation, it was observed that the best performance was shown by CPO-27-Ni that exhibits also an initial adsorption enthalpy of −13.5 kJ mol^{-1}, the highest yet observed for a MOF. Unfortunately, upon comparison of the hydrogen amounts stored at high pressure, the hydrogen capacities in these conditions are mostly dependent on the surface area and total pore volume of the material. This means that if control of MOF surface area can benefit the total stored amounts, only the presence of a great number of strong adsorption sites can make the (*P*,*T*) storage conditions more economically favorable. These observations lead to the prediction that efficient H_2 storage by physisorption can be obtained by increasing the surface density of strong adsorption sites.

Introduction

The safe and efficient storage of hydrogen is one of the greatest challenges in its use as an energy vector. Among the several envisaged technologies, molecular adsorption of dihydrogen on microporous solids has the advantage of being completely reversible and, at least in principle, simple.

Different classes of materials have been investigated as possible hydrogen adsorbents: these include carbons, zeolites, polymers, and metal−organic frameworks (MOFs).[1−9] Among them, MOF materials have attracted increasing attention because of their compositional flexibility and of their high crystallinity, which should guarantee the homogeneity of the material properties. Concerning the first point, their hybrid architecture, due to the combination of organic linkers and inorganic nodes, opens the possibility of designing and synthesizing a great variety of new porous materials with optimized pore volume, surface area, and coordination sites for the adsorption of hydrogen.

It is today well-known that some MOF materials are able to retain reversibly significant H_2 quantities (close to the DOE targets).[1−3] However, the storage pressure and temperature conditions (6.2 mass % and 7.0 mass % for IRMOF-20 and MOF-177, respectively, at 70 bar and 77 K) make their use economically unfavorable.[3] In order to improve the storage conditions, it is important to design new MOF materials not only having tailored pore dimension and large void volume but also incorporating strong adsorption sites, like for instance exposed metal ions which are known to reach binding enthalpies in the range 20−30 kJ mol^{-1}.[10] The tailoring of the interaction enthalpy is a crucial problem. In fact, binding enthalpies around 10 kJ mol^{-1} require cryogenic conditions to reach a significant adsorption, while binding enthalpies higher than 30 kJ mol^{-1} not only need thermal treatments to trigger hydrogen desorption at acceptable rates but also, more importantly, are connected with engineering problems. In fact, the target fixed by the DOE for the refueling time is the charge of 4 kg of hydrogen in 5 min: if we suppose an enthalpy of reaction of −30 kJ mol^{-1}

[†] Università di Torino.
[‡] SINTEF Materials and Chemistry.

(1) Dinca, M.; Dailly, A.; Liu, Y.; Brown, C. M.; Neumann, D. A.; Long, J. R. *J. Am. Chem. Soc.* **2006**, *128*, 16876–16883.
(2) Latroche, M.; Surble, S.; Serre, C.; Mellot-Draznieks, C.; Llewellyn, P. L.; Lee, J. H.; Chang, J. S.; Jhung, S. H.; Ferey, G. *Angew. Chem., Int. Ed.* **2006**, *45*, 8227–8231.
(3) Wong-Foy, A. G.; Matzger, A. J.; Yaghi, O. M. *J. Am. Chem. Soc.* **2006**, *128*, 3494–3495.
(4) Forster, P. M.; Eckert, J.; Chang, J. S.; Park, S. E.; Ferey, G.; Cheetham, A. K. *J. Am. Chem. Soc.* **2003**, *125*, 1309–1312.
(5) Spoto, G.; Vitillo, J. G.; Cocina, D.; Damin, A.; Bonino, F.; Zecchina, A. *Phys. Chem. Chem. Phys.* **2007**, *9*, 4992–4999.
(6) Zecchina, A.; Bordiga, S.; Vitillo, J. G.; Ricchiardi, G.; Lamberti, C.; Spoto, G.; Bjørgen, M.; Lillerud, K. P. *J. Am. Chem. Soc.* **2005**, *127*, 6361–6366.
(7) Germain, J.; Hradil, J.; Fréchet, J. M. J.; Svec, F. *Chem. Mater.* **2006**, *18*, 4430–4435.
(8) Collins, D. J.; Zhou, H. C. *J. Mater. Chem.* **2007**, *17*, 3154–3160.
(9) Thomas, K. M. *Catal. Today* **2007**, *120*, 389–398.
(10) Rowsell, J. L. C.; Yaghi, O. M. *Angew. Chem., Int. Ed.* **2005**, *44*, 4670–4679.
(11) Bhatia, S. K.; Myers, A. L. *Langmuir* **2006**, *22*, 1688–1700.
(12) Gutowska, A.; Li, L. Y.; Shin, Y. S.; Wang, C. M. M.; Li, X. H. S.; Linehan, J. C.; Smith, R. S.; Kay, B. D.; Schmid, B.; Shaw, W.; Gutowski, M.; Autrey, T. *Angew. Chem., Int. Ed.* **2005**, *44*, 3578–3582.

 10.1021/ja8007159 CCC: $40.75

for the exothermic charging process, the required power for keeping a constant storage vessel temperature is approximately 200 kW. Such heat transfer intensities represent a very severe engineering challenge for the hydrogen system as a whole. As a consequence, the heat evolved during the reaction would not be easily dispersed, and the introduction of a very powerful refrigerating system would be necessary to dissipate it. The problem of the optimal energetics of interaction for hydrogen storage materials has been considered in refs 11 and 12. On the basis of the previous considerations, a comparative study performed on MOFs characterized by the presence of different metal ions in the structure can be very useful to describe, at least at a qualitative level, the role of the cations in determining the cation/hydrogen interaction enthalpy. An evaluation of the number, distribution, and strength of specific interaction sites can be obtained by low-temperature IR spectroscopy of adsorbed hydrogen. In fact, although the ν(H−H) stretching of H_2 is IR inactive, once adsorbed on polarizing centers it undergoes a perturbation with disruption of the local symmetry and activation of the IR mode. Performing the adsorption and spectroscopic experiment at decreasing temperatures allows us to easily detect the temperature at which adsorption takes place with the appearance of the ν(H−H) IR bands. The resulting peaks are usually red-shifted, and their intensity is proportional to the strength of the interaction.[5,6,13–15]

In this study we have characterized the interaction of H_2 with three different MOFs having different topology, nature, and accessibility of the metal sites by using FTIR spectroscopy in the 300−20 K temperature range, in particular: (a) MOF-5 with inaccessible metal sites;[14] (b) HKUST-1 with accessible Cu^{2+} sites[13] (electronic configuration of bare Cu^{2+}: $3d^9$ $4s^0$); (c) CPO-27-Ni with exposed Ni^{2+} cations[16] (electronic configuration of bare Ni^{2+}: $3d^8$ $4s^0$). Isobaric H_2 adsorption experiments performed by decreasing the temperature in the 300−20 K range show that IR manifestations of adsorbed H_2 became detectable at a well-defined temperature (within approximation of ±10 K). This implies that the adsorption isobar must have a relatively sharp step at a definite temperature, allowing us to identify a well-defined onset temperature of the adsorption process. In this study, we have used the spectroscopic adsorption onset temperature as a quantitative indicator of the adsorption strength. This quantity also has the advantage of being intuitively correlated with the maximum operating temperature of a storage material.

The dependence of the temperature at which the adsorption starts and of the enthalpy of adsorption (obtained from the IR spectra)[17,18] on the shift of the H−H stretching frequency has been investigated. Electrostatic potential maps have been also evaluated for the three MOFs by means of density functional calculations to help the mapping and the location of the most charged regions in the MOF pores.

Materials and Methods

MOF Materials. The MOF samples in the form of powder, constituted by submicrometer-size particles suitable for IR measurements, were used in the form of self-supporting thin pellets.

MOF-5 material (Zn_4O(1,4-benzenedicarboxylate)$_3$) was obtained from $Zn(NO_3)_2 \cdot 6H_2O$ and 1,4-benzenedicarboxylate in a pure organic amine TEA and *N*,*N*′-dimethylformamide (DMF) solution following a synthesis procedure described in ref 19. The material so obtained presented a BET surface area of 565 $m^2\ g^{-1}$. The discrepancy with the values obtained by Yaghi et al.[10] has been discussed in depth in refs 13 and 20. This material needs activation in high vacuum at 523 K in order to eliminate H_2O and DMF.[14] A drawback of MOF-5 is that it easily hydrolyzes with a complete collapse of the structure,[21] as indicated by the decrease in the BET surface area from 565 to 47 $m^2\ g^{-1}$ after 6 weeks in air at RT reported by Panella et al.[22] and confirmed by us with a similar volumetric characterization reported in the Supporting Information as Figure S1. The HKUST-1 synthesis was performed in H_2O and EtOH by mixing $Cu(NO_3)_2 \cdot 3H_2O$ and benzene 1,3,5-tricarboxylic acid. The synthesis procedure is described in refs 13 and 23. Turquoise-blue crystals measured by X-ray powder diffraction indicated the high purity of the obtained material, and volumetric measurements gave a BET of 1800 $m^2\ g^{-1}$ (Langmuir surface area of 2257 $m^2\ g^{-1}$) for the as-synthesized material.[24] After 1 year of exposure in air, the BET surface area was 1150 $m^2\ g^{-1}$ (Langmuir 1524 $m^2\ g^{-1}$) The data are reported as Supporting Information, Figure S2. One of the advantages of using water as the solvent in HKUST-1 synthesis is that the material is quite robust toward moisture. This is possibly the reason why it shows a much larger stability in aging. The dehydrated form of HKUST-1 has been obtained upon activation in high vacuum for 1 h at 453 K. The CPO-27-Ni material was prepared from reaction of nickel(II) acetate and 2,5-dihydroxyterephthalic acid in a THF−water mixture to yield an ochre substance, $Ni_2(dhtp)(H_2O)_2 \cdot 8H_2O$, following a recipe reported in ref 16. X-ray powder diffraction data showed the high crystallinity of the sample for which a BET of 1200 $m^2\ g^{-1}$ has been evaluated (Langmuir surface area of 1315 $m^2\ g^{-1}$).[16,25] Water molecules are easily removed from this material that needs a thermal treatment at only 393 K. No substantial decrease in the BET surface area has been observed after 5 months in air. The isotherms related to the adsorption and desorption are reported in the Supporting Information section, as Figure S3 (BET of 840 $m^2\ g^{-1}$ and Langmuir surface area of 1090 $m^2\ g^{-1}$). As in the case of HKUST-1, the lower sensitivity to moisture of the CPO-27-Ni material with respect to MOF-5 can be related to the fact that it is synthesized in an aqueous medium. Table S1 summarizes the full set of data related to surface area and pore volume of the three samples as obtained for the fresh and the aged form.

IR Spectroscopy of H_2 Adsorption. Infrared spectroscopic measurements were performed using an *ad hoc* designed cryogenic cell allowing (i) the *in situ* high-temperature activation of the sample

(13) Bordiga, S.; Regli, L.; Bonino, F.; Groppo, E.; Lamberti, C.; Xiao, B.; Wheatley, P. S.; Morris, R. E.; Zecchina, A. *Phys. Chem. Chem. Phys.* **2007**, *9*, 2676–2685.
(14) Bordiga, S.; Vitillo, J. G.; Ricchiardi, G.; Regli, L.; Cocina, D.; Zecchina, A.; Arstad, B.; Bjørgen, M.; Hafizovic, J.; Lillerud, K. P. *J. Phys. Chem. B* **2005**, *109*, 18237–18242.
(15) Turnes Palomino, G.; Llop Carayol, M. R.; Otero Areán, C. *J. Mater. Chem.* **2006**, *16*, 2884–2885.
(16) Dietzel, P. D. C.; Panella, B.; Hirscher, M.; Blom, R.; Fjellvag, H. *Chem. Commun.* **2006**, 959–961.
(17) Otero Areán, C.; Turnes Palomino, G.; Garrone, E.; Nachtigallová, D.; Nachtigall, P. *J. Phys. Chem. B* **2006**, *110*, 395–402.
(18) Paukshtis, E. A.; Yurchenko, E. N. *Russ. Chem. Rev.* **1983**, *52*, 242–258.
(19) Huang, L. M.; Wang, H. T.; Chen, J. X.; Wang, Z. B.; Sun, J. Y.; Zhao, D. Y.; Yan, Y. S. *Microporous Mesoporous Mat.* **2003**, *58*, 105–114.
(20) Hafizovic, J.; Bjørgen, M.; Olsbye, U.; Dietzel, P. D. C.; Bordiga, S.; Prestipino, C.; Lamberti, C.; Lillerud, K. P. *J. Am. Chem. Soc.* **2007**, *129*, 3612–3620.
(21) Kaye, S. S.; Dailly, A.; Yaghi, O. M.; Long, J. R. *J. Am. Chem. Soc.* **2007**, *129*, 14176–14177.
(22) Panella, B.; Hirscher, M. *Adv. Mater.* **2005**, *17*, 538–541.
(23) Chui, S. S. Y.; Lo, S. M. F.; Charmant, J. P. H.; Orpen, A. G.; Williams, I. D. *Science* **1999**, *283*, 1148–1150.
(24) Xiao, B.; Wheatley, P. S.; Zhao, X. B.; Fletcher, A. J.; Fox, S.; Rossi, A. G.; Megson, I. L.; Bordiga, S.; Regli, L.; Thomas, K. M.; Morris, R. E. *J. Am. Chem. Soc.* **2007**, *129*, 1203–1209.
(25) Dietzel, P. D. C.; Johnsen, R. E.; Blom, R.; Fjellvåg, H. *Chem.—Eur. J.* **2008**, *14*, 2389–2397.

under high vacuum condition or in desired atmosphere and (ii) recording of IR spectra of the species adsorbed in the whole 300−20 K temperature interval while simultaneously measuring the gas-phase equilibrium pressure. This procedure allows us to obtain the site-specific adsorption enthalpy (VTIR method, see below) (iii) to perform FTIR adsorption/desorption experiments at fixed temperature, as low as ca. 20 K (estimated at the sample level), and variable H_2 pressure. A detailed description of the cryogenic cell (consisting of a modified closed circuit liquid helium Oxford CCC 1204 cryostat) is given elsewhere.[26] The FTIR spectra were collected in transmission mode on a thin self-supporting wafer (at 2 cm^{-1} resolution) on a Bruker Equinox-55 FTIR spectrometer equipped with an MCT detector whose sample compartment was modified *ad hoc* to accommodate the cryogenic IR cell.

Equivalent amounts of samples have been used to prepare MOF pellets with comparable weights and thicknesses. The samples were activated under high vacuum until complex dehydration (see the previous paragraph). H_2 (typically 50 mbar) was then dosed at 300 K from a vacuum manifold permanently attached to the IR cryogenic cell. A set of IR spectra have been collected lowering the temperature progressively from 300 to 20 K following the spectra evolution. The adsorption onset temperature T_{onset} was determined from each series by visual inspection, with an estimated accuracy of ±10 K. T_{onset} is therefore an empirical parameter which might be affected by instrument sensitivity and dynamics. However, the fact that the onset of detectable adsorption always occurs as a sharp and reproducible phenomenon operating with different sample end experimental setups suggests that T_{onset} is not significantly affected by these factors. The physical rationale for the rigorous definition of T_{onset} is that, although the coverage θ as a function of temperature T is a continuous function, it is possible to identify the maximum temperature at which localized adsorption occurs. At higher T, the adsorbate behaves like an almost free gas in the pores, only slightly perturbed by nondirectional dispersion forces. Upon lowering the temperature, the population π of site-bound polarized H_2 molecules builds up. π is also a continuous function of temperature, but it evidently displays detectable steps corresponding to sharp increases in single site populations upon temperature decrease. The concepts of order−disorder transition and phase transition in the adsorbate may apply to these systems. The statistical mechanics treatment of the phenomenon and its experimental verification with techniques other than IR spectroscopy are important issues of future research, but they are outside the scope of the present study. This experimental procedure (VTIR, Variable Temperature Infra-Red spectroscopic method)[17,18,27] has been already utilized for the weak adsorption of H_2 and other small molecules on a variety of materials,[5,17,28] and it allows us to evaluate the adsorption enthalpy. Details on the VTIR approach are described in the Supporting Information. The adsorption enthalpy is evaluated (in the Langmuir approximation) from the slope of the linear plot of $\ln A/(A_M - A)p$ vs $(1/T)$, where $A \equiv A(T)$ is the intensity of the selected IR manifestation of the adsorbed species as a function of the temperature T, A_M is the intensity of the same manifestation corresponding to the complete (1:1) filling of the adsorbing sites, and p is the equilibrium gas pressure. Once the lowest temperature was reached, samples have been allowed to equilibrate, until no further modification of the spectra was observable, revealing the absence of activated processes.[28] Finally, a set of measurements was performed at isothermal conditions (20 K) by decreasing the H_2 equilibrium pressure progressively. For the sake of conciseness, only the set of data obtained by lowering the temperature has been reported in this paper, while the isothermal spectra are presented in the Supporting Information.

Ultrahigh purity hydrogen has been used, and the gas has been passed through a molecular sieve trap immersed in liquid nitrogen before dosage.

Theoretical Calculations. The periodic single-point calculations were done at the BLYP/DN level (GGA functional) with the DMol^3 program (as embedded in Materials Studio 4.0, Accelerys Inc.)[29,30] on the unit cells of the three MOFs as obtained in literature from XRD refinement of their structures.[16,23,31]

Results and Discussion

Vibrational Spectroscopy of the H_2 Isomers. Before illustrating the IR manifestations of H_2 adsorbed on the MOF samples, it is useful to briefly summarize the basic spectroscopic properties of the dihydrogen molecule in the free (gaseous) state. These are dictated by the following facts:[32,33] (i) hydrogen molecules exist as two isomers differing for the orientation of the nuclear spins, i.e., para- (nuclear singlet state, $I = 0$) and ortho-H_2 (nuclear triplet state, $I = 1$); (ii) nuclear statistic confines the two spin isomers to different rotational states, characterized by even J (rotational quantum number) values for para- and by odd J values for ortho-H_2; (iii) the two isomers give rise to distinguishable spectroscopic manifestations in the Raman spectrum of normal H_2. The $v = 0 \rightarrow v = 1$ transition (v, vibrational quantum number) in para- (Q(0)) and ortho-H_2 (Q(1)) are at 4161 and 4155 cm^{-1}, respectively.[5] The $Q_1(0)$ and $Q_1(1)$ components shift to lower frequency (8−12 cm^{-1}) on passing from gaseous to liquid and solid H_2 and, as their separation increases, passing from 6 (gas) to 9 (solid) cm^{-1}. For what concerns the vibrational−rotational components, the lowest in frequency is the $S_1(0)$ at 4500 cm^{-1} for para-H_2 and the $S_1(1)$ at 4715 cm^{-1} for ortho-H_2.

In conclusion of this summary, it is worth recalling that although the equilibrium ortho/para ratio is a function of the temperature (e.g., it is 3:1 at 298 K and about 1:99 at 20 K), the interconversion of ortho-H_2 to the more stable para form is very slow even in the liquid state,[34,35] since it requires an inversion of nuclear spins. Faster interconversion can be promoted by spin catalysis (*vide* for instance ref 36 and references therein) through adsorption on metals such as tungsten and nickel and solids with surface-active and paramagnetic centers. Because the nuclear spin is reversed without breaking the H−H bond[35] and the two H_2 species have different spectroscopic features, we can follow the possible evolution of one species to the other during an IR experiment.

Structure of Investigated MOFs. The description and discussion of hydrogen reactivity toward these three different MOFs require a preliminary picture of their structure as they present a different topology, nature of the organic linkers, and accessibility of the metal sites.

Figure 1 summarizes all these aspects, comparing the three structures in terms of ligands and metal sites (top row), the unit cells (middle row), and the electrostatic potential in the pores

(26) Spoto, G.; Gribov, E. N.; Ricchiardi, G.; Damin, A.; Scarano, D.; Bordiga, S.; Lamberti, C.; Zecchina, A. *Prog. Surf. Sci.* **2004**, *76*, 71–146.
(27) Garrone, E.; Otero Areán, C. *Chem. Soc. Rev.* **2005**, *34*, 846–857.
(28) Gribov, E. N.; Bertarione, S.; Scarano, D.; Lamberti, C.; Spoto, G.; Zecchina, A. *J. Phys. Chem. B* **2004**, *108*, 16174–16186.
(29) *Materials Studio Modeling 4.0*; Accelrys Software Inc.: San Diego, CA, 2005.
(30) Delley, B. *J. Chem. Phys.* **1990**, *92*, 508–517.
(31) Eddaoudi, M.; Kim, J.; Rosi, N.; Vodak, D.; Wachter, J.; O'Keefe, M.; Yaghi, O. M. *Science* **2002**, *295*, 469–472.
(32) Herzberg, G. F. R. S. *Molecular spectra and molecular structure. I. Diatomic molecules*; D. Van Nostrand Company, Inc.: New York, 1950.
(33) Larin, A. V.; Jousse, F.; Leherte, L.; Vercauteren, D. P. *Chem. Phys. Lett.* **1997**, *274*, 345–353.
(34) Milenko, Y. Y.; Sibileva, R. M. *J. Low Temp. Phys.* **1997**, *107*, 77–92.
(35) Züttel, A. *Naturwissenschaften* **2004**, *91*, 157–172.
(36) Minaev, B. F.; Ågren, H. *J. Phys. Chem.* **1995**, *99*, 8936–8940.

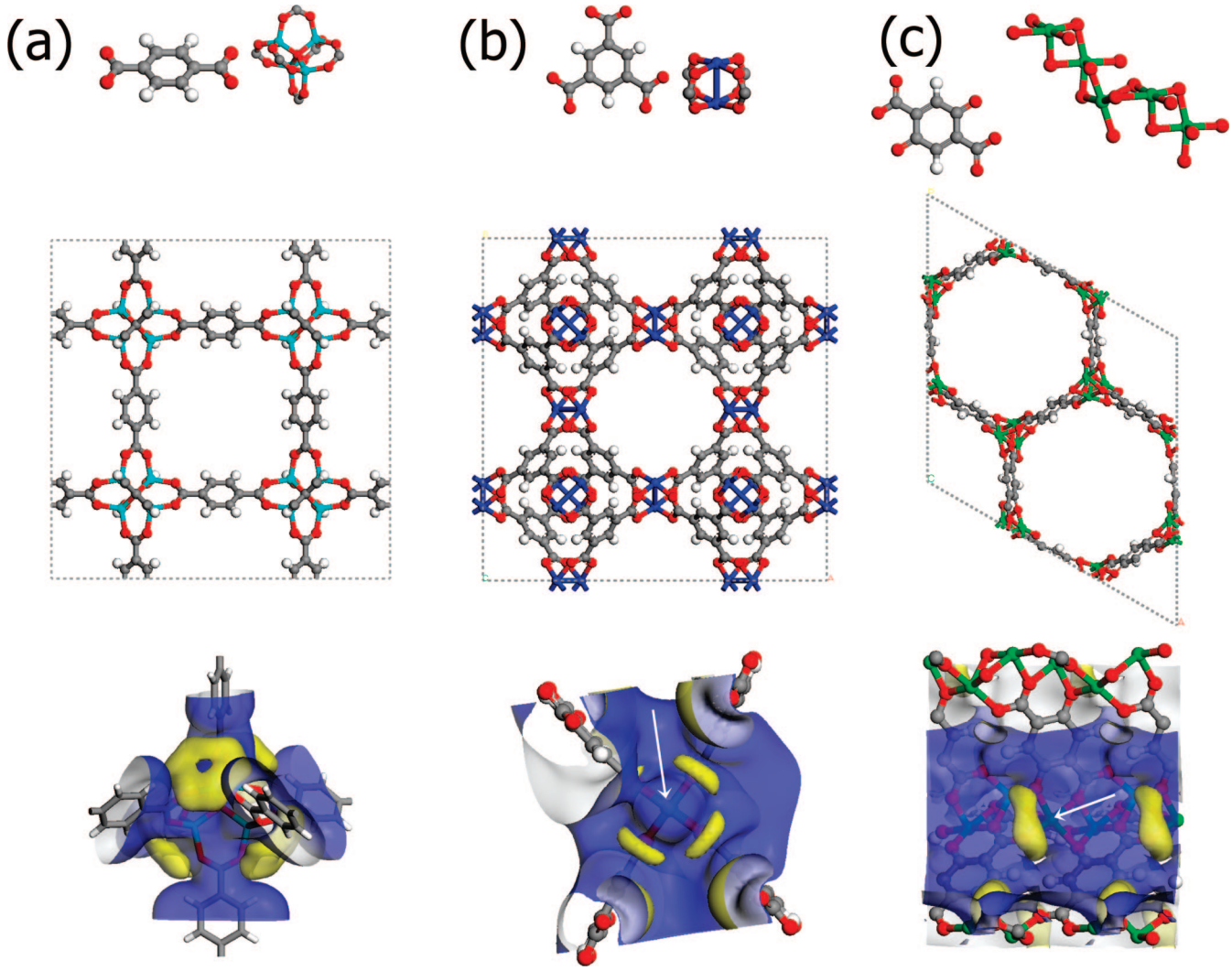

Figure 1. From top to bottom: organic linkers and inorganic nodes, unit cell, and a detailed view of the electrostatic potential map around the metal sites for (a) MOF-5, (b) HKUST-1, and (c) CPO-27-Ni. The C atoms are reported in gray; H atoms, in white; O, in red; Zn, in cyan; Cu, in blue; and Ni, in green. The electrostatic potential maps have been obtained at the BLYP/DN level on the X-ray resolved structure of MOF-5 (ref 31), HKUST-1 (ref 23), and CPO-27-Ni (ref 16). The isosurfaces corresponding to values of −0.015 and +0.015 au are reported in yellow and blue, respectively. White arrows indicate the coordination vacancies present in HKUST-1 and CPO-27-Ni.

(bottom row). The description of the latter is obtained with positive (blue) and negative (yellow) isosurfaces corresponding to ±.015 au. The calculated isosurfaces are located at a convenient distance (about 2.5 Å) from the atoms, representing a likely distance of coordination for hydrogen.[37]

Briefly, MOF-5 can be described as a cubic lattice of Zn_4O tetrahedra connected by 1,4-benzenedicarboxylate groups. Zinc atoms are completely coordinated, and therefore the metallic centers are not accessible to incoming probe molecules. For what concerns the polarity of the surface, the electrostatic potential map reported in Figure 1a shows a positive potential everywhere with the exception of a negative torus on the oxygen atoms of the carboxylates (directly linked to the Zn atoms).

The structure of HKUST-1 is defined by $Cu_2(CO_2)_4$ paddle-wheel units connected by 1,3,5-benzene tricarboxylate groups, forming a sequence of square cages (Figure 1b). In a previous publication it has been shown (using combined EXAFS, XANES, UV−vis, and IR spectroscopy) that the first coordination sphere of Cu^{2+} sites is significantly modified upon dehydration.[38] The shortening of the Cu−Cu distance and the distortion of the Cu−O bonds cause the appearance of coordinatively unsaturated Cu^{2+} ion sites overlooking the cages. The coordinative unsaturation of Cu^{2+} sites can be filled by adsorbed molecules, so that the dehydrated HKUST-1 represents an ideal material for gas adsorption and storage.[13,38] Analogously to what is observed for MOF-5, the electrostatic potential map obtained for HKUST-1 shows a potential everywhere positive with the exception of the oxygen regions. The arrow points toward the coordination vacancy at the Cu^{2+} sites.

CPO-27-Ni is part of a family of isostructural MOFs differing in the incorporated metal. Its structure can be described as a hexagonal packing of helical O_5Ni chains connected by 2,5-dihydroxyterephtalate linkers (Figure 1c).[16] This is an important difference with respect to the structure of the other two MOFs, characterized by 0-D metal oxide units, while here there are O_5Ni wires running parallel along the *c* axis of the crystal. The

(37) Sun, Y. Y.; Kim, Y. H.; Zhang, S. B. *J. Am. Chem. Soc.* **2007**, *129*, 12606–12607.

(38) Prestipino, C.; Regli, L.; Vitillo, J. G.; Bonino, F.; Damin, A.; Lamberti, C.; Zecchina, A.; Solari, P. L.; Kongshaug, K. O.; Bordiga, S. *Chem. Mater.* **2006**, *18*, 1337–1346.

resulting structure is a honeycomb-like network, which is a 1-D arrangement of parallel hexagonal channels with the metal chains at the vertex of the hexagons and the organic linkers at the faces (Figure 1c). All of the oxygen atoms of the ligand are involved in the coordination of nickel atoms. These account for five of the oxygen atoms coordinating each nickel atom, while the sixth coordinative position is occupied in the as-synthesized material by a water molecule which points toward the cavity. The channels of the honeycomb have a diameter of about 11 Å, and they are filled with water. It is possible to completely remove all the water present in the structure (both free water and Ni-coordinated water) upon a mild thermal treatment in vacuum (393 K). A detailed description of the effect of dehydration on the vibrational and electronic features will be reported in a separate paper.[39] The complete removal of the water molecules from this structure has been verified from the comparison of the IR spectra of the raw and dehydrated samples (Figure S6 of the Supporting Information). Because of the helical arrangement of the NiO_5 units, the nearest Ni atoms are exposed in different channels: for this reason the smallest distance between nearest Ni ions exposed in the same channel is 6.8 Å. All the Ni^{2+} ions are identical with respect to the first coordination sphere, showing five oxygen atoms that slightly differ from each other (see Figure S7a in the Supporting Information), in particular, two O_{cs} (oxygens from two different carboxylate units, each of them shared with another Ni ion), one O_{cu} (oxygen from one of the previous carboxylate units, not shared with another Ni ion), and two O_{OHs} (oxygens from the deprotonated OH group of two other linkers, each of them shared with another Ni ion). This heterogeneity is reflected in the electrostatic potential map: in fact, the negative isosurface is due only to the contribution of two O_{OHs} and the O_{cu} (yellow area in Figure 1c). An orthogonal view with respect to the channel is reported in Figure S7b where it is evident that each Ni ion protruding in a channel is associated with one yellow area given by a contribution of one O_{OHs} and the O_{cu}. The other two oxygens (O_{cs}) are much less electronegative and do not contribute to the negative isosurface reported in Figure 1c, while the second O_{OHs} contributes to a negative surface exposed to a different channel (see Figure S7b). Incoming molecules would experience a positive electrostatic potential along the MOF channels; the arrow evidences the coordination vacancy of Ni^{2+} sites.

IR Spectra of Adsorbed H_2. The Raman stretching frequency of H_2 gas that we consider as reference for the unperturbed molecule is 4161 cm^{-1} (para-H_2). Hydrogen interaction with surfaces implies the appearance of IR bands that are usually red-shifted proportionally to the interaction strength. Summarizing the results presented in the literature for the H_2 adsorption on high surface area materials, the type of interaction can be roughly recognized on the basis of the $\tilde{\nu}$(H−H) red shift. In particular it has been observed that very weak H_2 adsorptions are associated with bands at $\geq$4120 cm^{-1} ($|\Delta\tilde{\nu}| \leq 40$ cm^{-1}) in the case of organic[5] or inorganic[6] microporous and mesoporous materials. This spectral range includes also the features associated with liquid-like and physisorbed hydrogen. Conversely, when the interaction occurs thanks to polarizing centers like cations,[17,40,41] anions, or anion/cation couples,[43] the spectroscopic features strongly depend on the interaction site (charge/radius value),[17] presence of *d* orbitals,[40] and first coordination sphere (that influences the ionicity of the framework).[6,44] This causes a larger spread of values that can appear from about 4120 down to 3900 cm^{-1}. The data described in this work refer to both families of interaction.

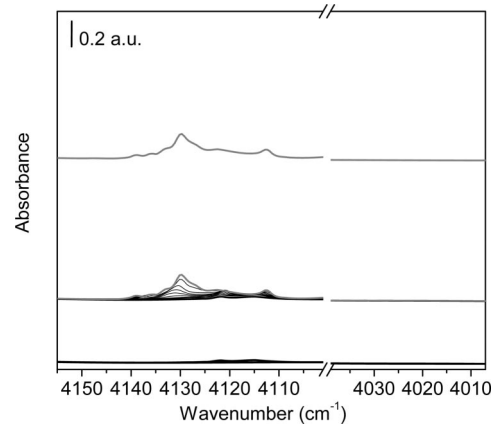

Figure 2. FTIR spectra (background subtracted) of H_2 adsorbed on MOF-5: lower section reports the spectra obtained during the first part of the sample cooling (300−80 K); middle section reports the spectra obtained during the final part of the sample cooling (from 80 K down to 20 K, bold light gray curve); upper section reports the effect of the contact time at 20 K and constant equilibrium pressure for 2 h. No changes have been observed during this contact time. Bold light gray is the same as that in the middle section. a.u. = absorbance units.

The spectroscopic results which will be discussed in the following have been performed under isobaric conditions (constant pressure and decreasing temperature).

MOF-5. The VTIR spectra recorded for the adsorption of H_2 on MOF-5 are reported in Figure 2.

The first IR signals (doublet at 4121 and 4112 cm^{-1}) appear at 105 K. On the basis of literature experiments concerning H_2 adsorption on a variety of solids[6] this doublet is assigned to para- and ortho-H_2 adsorbed on weak polarizing defects (e.g., OH groups). Comparison with the H_2 spectra on ZnO rules out any assignment to H_2 interacting with exposed Zn^{2+}.[45] Upon decreasing the temperature a new band appears at 4128 cm^{-1} ($\Delta\tilde{\nu} = -33$ cm^{-1}) which subsequently grows and moves to 4130 cm^{-1}. This band can be assigned to para-H_2 in interaction with the apolar walls of MOF-5.[14] The intensities of the bands at 4112 and 4130 cm^{-1} have been measured as a function of *T*. The ΔH_{ads} evaluated with the VTIR method[17,18] for the 4112 cm^{-1} band was −7.4 kJ mol^{-1}, whereas a value of −3.5 kJ mol^{-1} was obtained for the 4130 cm^{-1} peak. These values well compare with the adsorption enthalpy of 4.7−5.2 kJ mol^{-1} reported by Kaye and Long for H_2 adsorption on MOF-5.[46] The differences between them can be explained by the different ways they have been obtained, being the latter values an average enthalpy between the different species involved in the interaction

(39) Bonino, F.; Chavan, S.; Vitillo, J. G.; Groppo, E.; Agostini, G.; Lamberti, C.; Dietzel, P. D. C.; Prestipino, C.; Bordiga, S. *Chem. Mater.* **2008**, in press.
(40) Spoto, G.; Gribov, E.; Bordiga, S.; Lamberti, C.; Ricchiardi, G.; Scarano, D.; Zecchina, A. *Chem. Commun.* **2004**, 2768–2769.
(41) Vitillo, J. G.; Damin, A.; Zecchina, A.; Ricchiardi, G. *J. Chem. Phys.* **2005**, *122*, 114311.
(42) Vitillo, J. G.; Damin, A.; Zecchina, A.; Ricchiardi, G. *J. Chem. Phys.* **2006**, *124*, 224308.
(43) Torres, F. J.; Vitillo, J. G.; Civalleri, B.; Ricchiardi, G.; Zecchina, A. *J. Phys. Chem. C* **2007**, *111*, 2505–2513.
(44) Bordiga, S.; Garrone, E.; Lamberti, C.; Zecchina, A.; Otero Areán, C.; Kazansky, V. B.; Kustov, L. M. *J. Chem. Soc., Faraday Trans.* **1994**, *90*, 3367–3372.
(45) Scarano, D.; Bertarione, S.; Cesano, F.; Vitillo, J. G.; Zecchina, A. *Catal. Today* **2006**, *116*, 433–438.
(46) Kaye, S. S.; Long, J. R. *J. Am. Chem. Soc.* **2005**, *127*, 6506–6507.

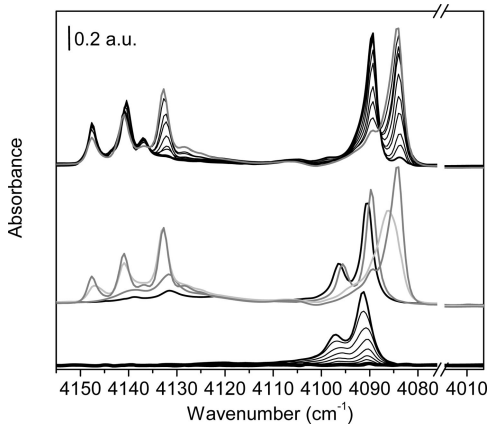

Figure 3. FTIR spectra (background subtracted) of H_2 adsorbed on HKUST-1: lower section reports the spectra obtained during the first part of the sample cooling (300−80 K); middle section reports the spectra obtained during the final part of the sample cooling (from 80 K down to 20 K, bold gray curve); upper section reports the effect of the contact time at 20 K and constant equilibrium pressure. Upper bold gray line is the same as that in the middle section; bold dark gray line, after 30 min of contact at 20 K; black lines, intermediate contact times. No further changes have been observed for longer contact times (10 h). a.u. = absorbance units.

at a certain value of the coverage, whereas the ΔH_{ads} obtained by the VTIR method are characteristic of one specific adsorbed species. Calculations reported previously[14] for H_2 adsorption on the MOF-5 oxidic part (MP2/aug-cc-pVDZ) give a binding energy in the 2.0−3.2 kJ mol^{-1} interval, whereas calculations for the H_2 interaction with the organic part give a BE of 4.3 kJ mol^{-1}.[5] Both computational values are closer to the enthalpy of the 4130 cm^{-1} species than to the enthalpy associated with the 4112 cm^{-1} species. These low energy values agree with the fact that these bands are truly reversible upon outgassing at 20 K (see Figure S8 of the Supporting Information). The spectra collected at the lowest temperature show the appearance of weak bands at 4146 and 4138 cm^{-1}, assigned to liquid-like H_2 in the MOF-5 channels (para- ad ortho-H_2 respectively). This assignment is justified by the fact that they have been observed with little variations in all IR spectra recorded at 20 K on hydrogen adsorbed on different microporous materials.[6,13,14,38,47] The low intensity of the para component of the liquid-like phase is an indication that no ortho−para catalyzed reaction happens on this material. Moreover, no ortho- to para-H_2 conversion was observed even after contact for 2 h at 20 K. This conclusion is confirmed by examination of the H_2 rotovibrational region (Figure S9 of the Supporting Information) where very weak signals are clearly visible only for the ortho isomer, while the para species are hardly distinguishable. This result is different from those observed on other microporous materials and the other MOFs studied in the present paper.[5]

HKUST-1. Figure 3 (bottom and central parts) reports the IR spectra recorded under sample cooling from 300 to 20 K after dosing of 50 mbar of H_2. Figure 3 (top part) refers to the spectra collected at 20 K during the sample equilibration.

The IR bands due to adsorbed H_2 belong to two separated groups: the bands of the first group have frequencies in the 4080−4100 cm^{-1} interval, while the bands of the second group fall in the 4150−4120 cm^{-1} interval (i.e., the same interval observed in MOF-5). Following the rough distinction reported at the beginning of the paragraph: the first group of bands belongs to H_2 interacting with coordinatively unsaturated Cu^{2+}, while the second group is due to H_2 more weakly adsorbed on the organic part.

The first IR signals related to adsorbed H_2 were observed at 110 K (peaks at 4097 and 4090 cm^{-1}) and grow in a parallel way upon temperature decrease. The observed frequency separation, intensity ratio, and coverage dependence (*vide infra*) allow the assignment of this doublet to para-H_2···Cu^{2+} and ortho-H_2···Cu^{2+} complexes.[13,38] This assignment is also supported by recent results of a neutron diffraction study of D_2 sorption on HKUST-1 that indicates the Cu^{2+} sites as the most favorable for adsorption.[48]

The interaction enthalpy of H_2 in these H_2···Cu^{2+} complexes has been estimated by means of the VTIR method. An adsorption enthalpy of −10.1 kJ·mol^{-1} was calculated for the 4097 cm^{-1} peak. An enthalpy of about 10 kJ·mol^{-1} is rather remarkable. Highly exposed monovalent cations in some zeolites[6,17,27,40] gave similar interaction enthalpies. A similar value (9.5 kJ mol^{-1}) was reported for H_2···Cu^{2+} complexes in sodalite type Cu-MOFs.[49] Frequency shifts and interaction enthalpy found in HKUST-1 suggest that the Cu^{2+} ion behaves like a purely polarizing center where *d*-electrons do not effect the interaction with H_2. In this sense Cu^{2+} is similar to alkaline earth cations. Turnes Palomino et al.[15] found a ΔH_{ads} of −17.5 kJ mol^{-1} for adducts formed upon interaction with highly exposed Mg^{2+} inside a Na−Mg−Y zeolite. As Cu^{2+} and Mg^{2+} have a similar charge to radius ratios,[50] the smaller value found for HKUST-1 can be explained by the shielding role of the oxygen atoms of the carboxylate units.

Upon decreasing the temperature to 20 K (central curves in Figure 3), the intensity of the doublet at 4097 and at 4090 cm^{-1} progressively decreases while a new adsorption at lower $\tilde{\nu}$ grows up at 4084 cm^{-1}. The frequency maximum of the new adsorption is gradually changing with coverage, and only at the end of stage two a final situation characterized by a peak at 4084 cm^{-1} with a shoulder at 4089 cm^{-1} is observed. The shape of this doublet is very similar to the original doublet at 4097−4090 cm^{-1}. During the gradual transformation of the vibrational properties of H_2 adsorbed on Cu^{2+} ions, the growth of bands due to H_2 (ortho and para) interacting with the organic part of the framework (presumably the phenyl rings) is occurring in the 4120−4150 cm^{-1} range.

In particular, the growth of a peak in the 4130−4136 cm^{-1} range (with the corresponding ortho component at 4128 cm^{-1}) seems to be specifically correlated with the shift of the new H−H band of the Cu^{2+}/H_2 complexes.

These results can be most plausibly explained on the basis of Scheme 1.

Following Scheme 1 the gradual change in the $\tilde{\nu}$(H−H) complexes in the 4090 cm^{-1} range is due to the gradual modification of the surrounding medium due to the filling of the weak phenyl sites. This gradual shift of the $\tilde{\nu}$(H−H) at 4090 cm^{-1} is even more clearly evidenced on the experiment conducted at constant *T* (20 K) and variable pressure (see Supporting Information Figure S10). This continuous modification is always observed when the surrounding of a given oscillator is gradually modified by the filling of adjacent and more distant sites. The observed downward shift (about 6 cm^{-1})

(47) Ricchiardi, G.; Vitillo, J. G.; Cocina, D.; Gribov, E. N.; Zecchina, A. *Phys. Chem. Chem. Phys.* **2007**, *9*, 2753–2760.
(48) Peterson, V. K.; Liu, Y.; Brown, C. M.; Kepert, C. J. *J. Am. Chem. Soc.* **2006**, *128*, 15578–15579.
(49) Dinca, M.; Han, W. S.; Liu, Y.; Dailly, A.; Brown, C. M.; Long, J. R. *Angew. Chem., Int. Ed.* **2007**, *46*, 1419–1422.
(50) Shannon, R. *Acta Crystallogr., Sect. A* **1976**, *32*, 751–767.

Scheme 1

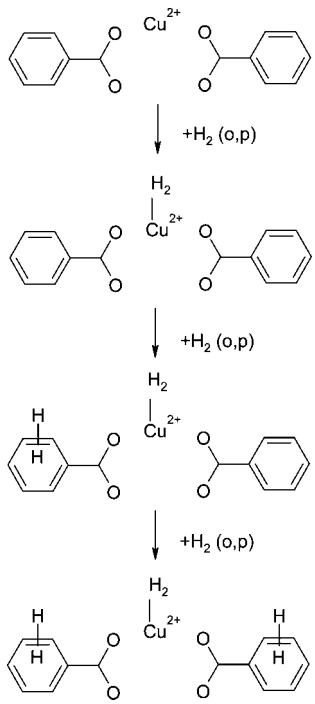

is in agreement with this hypothesis because it is similar to that of a not very dense liquid phase. Notice that on passing from gas to liquid H_2 the shift is of 7−9 cm^{-1}.[5] It is quite conceivable that during this process the $Cu^{2+}\cdots Cu^{2+}$ and the $Cu^{2+}-O$ distances are also slightly modified because the framework is relaxing upon hydrogen adsorption. Due to the small involved enthalpies, this relaxation is certainly very modest.

On the basis of the proposed scheme, the two bands at 4141−4148 cm^{-1} appearing at the later stage are assigned to liquid-like H_2 in the second adsorbed layer. The two bands correspond to ortho- and para-H_2, respectively. Due to the small frequency difference between these species, dipole−dipole coupling is not excluded which makes the whole spectrum very complex and difficult to assign in detail.

The successive set of spectra (top part of Figure 3) has been obtained waiting for sample equilibration at 20 K at constant pressure. In this case, the effect of this equilibration was completely different from that observed for MOF-5. In the first 30 min at 20 K, we observe the selective decrease of the band at 4084 cm^{-1}, the parallel growth of the component at 4089 cm^{-1} (clear isosbestic point at 4087 cm^{-1}), the disappearance of the band at 4133 cm^{-1}, and the small increase of all the others components (4137, 4140, and 4148 cm^{-1}). These changes are completed within approximately 30 min, while no changes have been monitored in the following hours. These time-dependent spectral changes are associated with conversion of ortho- into the more stable para-H_2. The nearly complete conversion of ortho-H_2 into the more stable para form contributes also to the dramatic change in the intensity ratio of the two bands at 4084 and at 4089 cm^{-1}. The time scale for the extensive ortho/para-H_2 conversion is actually much shorter than that reported for pure H_2 and for H_2 in other microporous materials at comparable temperatures (see refs 51 and 47, respectively). We can therefore

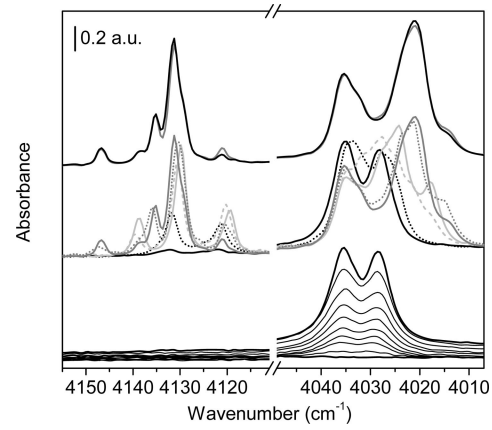

Figure 4. FTIR spectra (background subtracted) of H_2 adsorbed on CPO-27-Ni: lower section reports the spectra obtained during the first part of the sample cooling (300−78 K); middle section reports the spectra obtained during the final part of the sample cooling (from 72 K down to 20 K, bold light gray curve). Upper section reports the time evolution at 20 K and constant equilibrium pressure. Bold light gray is the same as in the middle section, bold dark gray line after 30 min of contact at 20 K; black lines, intermediate contact times. No further changes have been observed for longer contact time (10 h). a.u. = absorbance units.

conclude that Cu^{2+} in HKUST-1 acts as a spin catalyst, similarly to other oxidic materials containing paramagnetic impurities.[35] This conclusions is in full agreement with the results obtained in the 4800−4400 cm^{-1} region, where the vibro-rotational peaks due to para-H_2 (complex absorption centered at 4470 cm^{-1}) are more intense than those related to the ortho-rotational features (band at 4630 cm^{-1}, see Figure S11). Note that the rotational contributions start to develop only in presence of a significant amount of weakly adsorbed hydrogen (bands in the range 4150−4120 cm^{-1}). The lower rotational freedom of H_2 when adsorbed on the metal sites rather than on the organic linkers in MOFs has been observed by Forster and co-workers in INS experiments involving H_2 adsorption on Ni-based metal−organic frameworks.[4,52] In fact, they observe that when hydrogen is adsorbed on the metal centers, the reorientation of the dihydrogen ligand is approximately constrained to a plane on account of the side-on coordination to the metal so that the molecule has only one rotational degree of freedom. On the contrary, when H_2 is less strongly adsorbed (as, for example, in the interaction with the organic part of the framework), the system can be described as a hindered rotor with two rotational degrees of freedom.[4,52]

CPO-27-Ni. The FTIR spectra recorded from 300 to 20 K are presented in Figure 4 (bottom and central parts). As observed in previous cases, the adsorption of H_2 results in the appearance of bands in two distinct regions (4010−4040 and 4110−4150 cm^{-1}). The first region is associated with H_2 interacting primarily with Ni^{2+}, while the second region is associated with H_2 adsorbed on ligands. The first noticeable novelty observed in this material is the high temperature (180 K) at which H_2 adsorption is first observed during sample cooling. Evidence of early H_2 interaction with surface Ni^{2+} sites is given by the appearance of the doublet at 4035 and 4028 cm^{-1} that show a parallel intensity growth. Similar frequencies were previously observed only in the case of highly uncoordinated ions such as

(51) Häussinger, P.; Lohmüller, R.; Watson, A. M. Hydrogen. In *Ullmann's Encyclopedia of Industrial Chemistry*, 5th ed.; John Wiley & Sons: 1989; Vol. A*13*, pp 297−442.

(52) Forster, P. M.; Eckert, J.; Heiken, B. D.; Parise, J. B.; Yoon, J. W.; Jhung, S. H.; Chang, J. S.; Cheetham, A. K. *J. Am. Chem. Soc.* **2006**, *128*, 16846–16850.

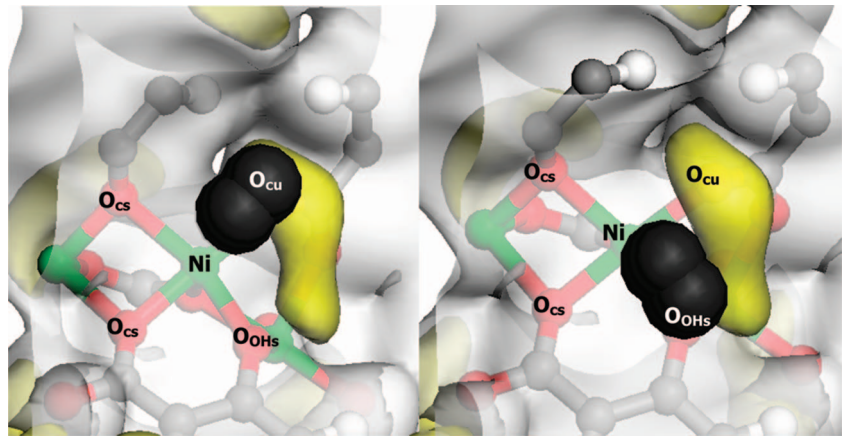

Figure 5. H_2 adsorption on the Ni site: pictorial representation of two likely $Ni^{2+}\cdots H_2$ adducts. The H atoms of the H_2 molecule are represented as black spheres. Yellow areas correspond to a −0.015 au value of the electrostatic potential. Labels of atoms are described in the text.

Fe(III) ions in Fe_2O_3 nanoparticles,[53] Al(III) on edges and corners[54] in γ-Al_2O_3, or Zn(II) in ZnO.[45] The novelty in the case of CPO-27-Ni is the fact that those strong adsorption sites are present as regular bulk structural units and not as defects as in the previously mentioned oxides. In this case, the large shift is due to the electronic structure of the coordination sites. The presence of *d*-electrons in the valence sphere makes the interaction with H_2 not of a purely electrostatic nature, involving charge transfer from the H_2 to the metal. Moreover as the average metal−O distance in CPO-27-Ni (1.99 Å)[39] was found to be larger than that in HKUST-1 (1.94 Å)[38] and as Ni possesses a higher charge/ionic radius ratio than Cu, the Ni^{2+} ions are expected to have a higher polarization power than the Cu^{2+} also on the electrostatic point of view. The separation between the two maxima (7 cm^{-1}) would be consistent with the presence of both ortho- and para-hydrogen in a 1:1 proportion. If this was the case, a gradual erosion of the ortho component (band expected at 4028 cm^{-1}) would be observed upon lowering the temperature. Unfortunately the spectra evolution in the 72−20 K interval (central part of Figure 4) is too complex to confirm this kind of speculation. However, if the ortho−para conversion was relevant already at very moderate temperature (180 K), the para isomer should be significantly more intense in the spectra obtained on desorption (Figure S12 bottom part). But this is not the case as the band at 4035 cm^{-1} is only slightly more intense than that at 4028 cm^{-1}. This observation implies that the two peaks are not due to ortho/para-H_2 but that we have to consider the presence of two very similar $Ni^{2+}\cdots H_2$ complexes. As described in the previous section, all the Ni^{2+} ions are identical with respect to the first coordination sphere, showing five oxygen atoms that slightly differ from each other. We think that this heterogeneity in the first coordination sphere could explain the presence of two bands observed at low coverage as due to the formation of two similar but distinct adducts. A pictorial representation of these two adducts is shown in Figure 5. In both cases H_2 is directly interacting with the nickel cation and with O_{cu} (Figure 5a) or O_{OHs} (Figure 5b), respectively. Deeper insight into these two oxygens reveals that O_{cu} is slightly more negative than O_{OHs}. As it has been observed that small variation of the Lewis basicity in a cation/anion couple results in a significant variation of the $\Delta\tilde{\nu}$(H−H),[43,44] the two maxima (4035 and 4028 cm^{-1}) can be ascribed to complexes involving the O_{OHs} and O_{cu}, respectively. We suggest that the Ni sites can form two complexes with similar adsorption enthalpy but with different geometries. It is in fact well demonstrated by theoretical calculations that different interaction geometries can cause different $\Delta\tilde{\nu}$(H−H) even in the case of similar binding energies.[43] For this reason the VTIR method has been applied to both bands, giving a value for the adsorption enthalpy of −13.5 kJ mol^{-1}, which is one of the highest reported for hydrogen so far.[15,47] In particular, this is the highest value yet observed for a microporous metal−organic framework, also compared to other Ni-containing MOFs (−9.1 kJ mol^{-1} for **1**-Ni^{2+} and −10.4 kJ mol^{-1} for $NaNi_3(OH)(SIP)_2$).[8,52,55]

Decreasing the temperature, the formation of bands in the 4150−4110 cm^{-1} range is clearly observed due to the adsorption at organic linkers, while the previous doublet undergoes a continuous transformation into a more complex system of bands progressively extending in range down to 4010 cm^{-1}. The spectral evolution is very complex; however it is possible to recognize a "step by step" red shift of the doublets (as already observed in case of HKUST-1) that can be interpreted in terms of the gradual modification of the surrounding medium due to the filling of adsorption sites at the organic linkers. The new main component results downward shifted by 7 cm^{-1} with respect to the original position, a value expected for a transition from the gas to liquid phase.[5] It is sensible to assume that during this process the $Ni^{2+}\cdots O\cdots Ni^{2+}$ distances are also slightly modified because of framework relaxation upon hydrogen adsorption. The final spectrum of this series is again characterized by two main absorptions with maxima at 4035 and at 4020 cm^{-1} and a shoulder at 4033 and 4012 cm^{-1}, respectively. The complexity of the spectra is increased by some ortho−para conversion of hydrogen, even if the phenomenon is less evident than in the case of HKUST-1. Starting from 65 K, the roto-vibrational region of hydrogen shows undoubtedly the appearance of a peak at 4440 cm^{-1} which is ascribable to para-H_2 (see Figure S13 in the Supporting Information). It is noteworthy that this band is really sharp with respect to the corresponding one observed on similar systems, e.g., HKUST-1 and MOF-5. The complexity of the evolution of the bands associated with hydrogen interacting with Ni^{2+} sites might be the result of the presence of substituents of different natures on the benzene rings (carboxylate and alcoholate), which can give rise to slightly

(53) Berlier, G.; Gribov, E. N.; Cocina, D.; Spoto, G.; Zecchina, A. *J. Catal.* **2006**, *238*, 243–249.
(54) Spoto, G., manuscript in preparation.
(55) Dinca, M.; Long, J. R. *J. Am. Chem. Soc.* **2007**, *129*, 11172–11176.

different situations. Finally, it can be noted that absorptions are quite broad with respect to those observed for HKUST-1. Parallel to this complex spectra evolution, in the higher frequency range (4110 to 4150 cm^{-1}) many narrow peaks appeared that show a complex evolution during the cooling process. Starting with a doublet at 4132 and at 4121 cm^{-1}, upon decreasing the temperature we observe the additional growth of a band at 4138 cm^{-1} and then the appearance of two new components at 4146 and at 4135 cm^{-1} accompanied by the erosion of the bands at 4138 cm^{-1} and at 4121 cm^{-1}. Shifts in the range 20−40 cm^{-1} indicate that these bands are associated with the formation of only slightly perturbed species. The situation is very similar to what has been observed in the case of HKUST-1. However, we note that the main component is about 10 cm^{-1} more red-shifted with respect to that case. A possible explanation for this difference is the fact that in CPO-27-Ni the channel structure allows to optimize the geometry of the second and third hydrogen layers and/or that the presence of the available extra oxygen in the linker can act as a further polarizing center. It has been shown that H_2 interaction with anions perturbs the H−H frequency more strongly than cations at the same energy of interaction.[42]

Nearly no changes are observed in the spectra after 30 min (see upper part of Figure 4), indicating that no further ortho−para conversion is observed after leaving the system to equilibrate for longer time at the lowest temperature. In the end, at the highest coverage the spectrum is characterized by two main components in the high frequency range (4147 and 4138 cm^{-1}) related to a liquid-like phase in the pores of CPO-27-Ni, while in the low frequency range the spectrum is dominated by a triplet at 4035, 4131, and 4020 cm^{-1}. Note the very high intensity of this spectrum as compared with the spectra collected at both the lowest T and highest coverage in cases of MOF-5 and HKUST-1.

Unlike in MOF-5 and HKUST-1, the adsorption was irreversible at 20 K in CPO-27-Ni and it was necessary to heat the material up to 50 K in order to desorb H_2 completely. The spectra evolution obtained during the desorption process is very similar to the series of spectra collected on adsorption (see Figure S12 of the Supporting Information), with the only difference that at the lowest coverage the band at 4035 cm^{-1} is slightly more intense than the band at 4028 cm^{-1}. This implies that ortho−para conversion in this material is not catalyzed.

Comparative Evaluations of Dihydrogen/MOF-5, HKUST-1, and CPO-27-Ni Interaction. The interaction of hydrogen with the adsorption centers is associated with the following consequences:

(a) the magnitude of the stretching frequency shift increases on passing from aromatic groups to Cu and Ni centers;

(b) the intensities of the $\tilde{\nu}$(H−H) peaks show the same behavior, due to an increase of the extinction coefficient.

(c) The onset temperature T_{onset} of the first dihydrogen complex formation increases on going from MOF-5, HKUST-1, to CPO-27-Ni.

To quantify these observations, the dependence of T_{onset} on $\Delta\tilde{\nu}$ (the shift in the H−H stretching frequency) has been investigated. As it can be seen in Figure 6, T_{onset} shows a linear dependence on $\Delta\tilde{\nu}$ (red line): this means that $\Delta\tilde{\nu}$ can be taken as an indication of the T_{onset} also when this quantity is not available. In particular CPO-27-Ni shows not only the larger shift of the H−H stretching frequency but also the highest onset temperature at which the adsorption starts (180 K), followed by HKUST-1 and MOF-5, for which the adsorption starts at

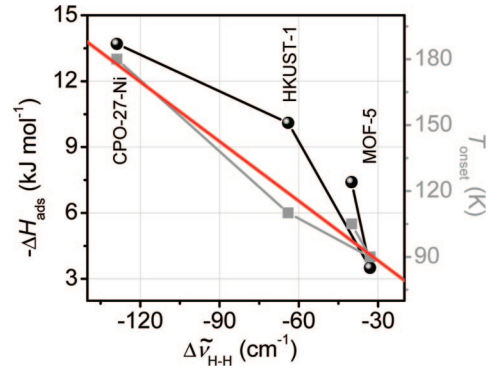

Figure 6. Dependence of the adsorption enthalpy (ΔH_{ads}, black circle) and of the temperature at which the H_2 complexes are observed (T_{onset}, gray squares) on the corresponding shift of the H−H stretching frequency for the three MOFs under investigation. Para-H_2 has been used as reference. The red line corresponds to the linear regression of the T_{onset} data: $y = mx + q$ where $m = -0.90436$ K cm and $q = 61.15506$ K ($r^2 = 0.9694$ and max. dev. = 8.57425). For CPO-27-Ni, the barycenter of the 4028 and 4035 cm^{-1} bands has been considered.

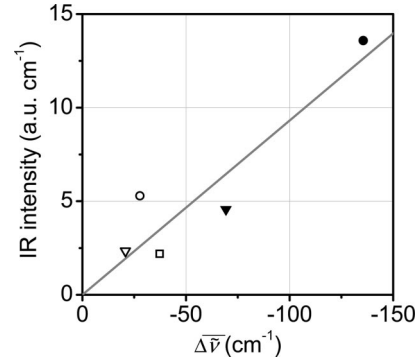

Figure 7. Dependence of the intensity of the bands on the average frequency shift $\Delta\bar{\tilde{\nu}}$. The intensity has been evaluated as the integral of the bands area for MOF-5 (square), HKUST-1 (triangles), and CPO-27-Ni (circles) obtained at the highest coverage for the two main families of bands associated, respectively, to metal-dihydrogen complexes (filled scatters) and H_2 adsorption on the organic parts (empty scatters). The straight line is the result of a linear regression on the data: $y = ax$, with $a = -0.093\,109$ au·cm^{-1}, max dev: 2.6938, $r^2 = 0.861\,66$. The $\Delta\bar{\tilde{\nu}}$ has been calculated with respect to the para-H_2.

the lowest temperature (105 K on the defects, 80 K on the MOF-5 walls). Similarly, the adsorption enthalpy is strongly correlated with frequency shifts (Figure 6), and the CPO-27-Ni, with its 13.5 kJ mol^{-1}, results in being the most active material toward H_2. These relationships can be ascribed to the different natures and accessibilities of the metal sites. In fact the least reactive sample is MOF-5, a material not containing exposed metal sites. On the contrary HKUST-1 and CPO-27-Ni, having well exposed metal sites with coordinative vacancies, show distinctly higher T_{onset}. The corresponding shifts in the H−H frequencies are noticeable and are an indication of the large perturbation that the H_2 molecule experiences on adsorbing at the metal sites. On the basis of a purely energetic evaluation, the best performance is shown by CPO-27-Ni.

The IR spectra shown in Figures 2, 3, and 4 have been reported with the same scale in order to underline the dramatic differences concerning the intensity and frequency of the bands. Figure 7 reports the intensities of the aromatic and metal complexes in the spectra at the highest coverage as a function of the average frequency shift $\Delta\bar{\tilde{\nu}}$ for the three MOFs. The values reported in ordinate are normalized by

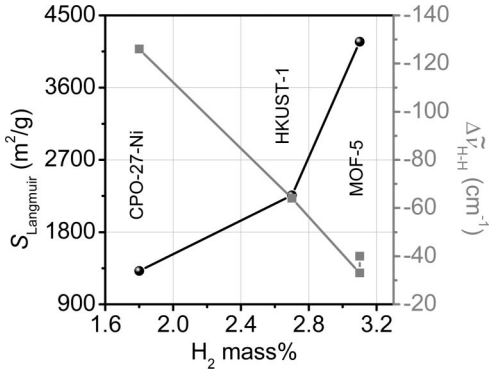

Figure 8. Dependence of the Langmuir surface area ($S_{Langmuir}$, black circle) on the adsorbed H_2 amounts at 77 K and 45 bar (volumetric values) for the three MOFs under investigation. Values taken from the literature: MOF-5,[3] HKUST-1,[3] and CPO-27-Ni.[16] The dependence of the H−H shift for the most energetic complexes on the hydrogen uptake is also shown (para-H_2 has been used as reference, gray squares). For CPO-27-Ni, the barycenter of the 4028 and 4035 cm^{-1} bands has been considered.

considering that each metal interacts directly with one hydrogen molecule while each benzene ring interacts with two H_2. It is striking that the IR intensity of the H_2 complexes on the exposed Ni metal sites are almost three times more intense with respect to the $H_2\cdots Cu^{2+}$ complexes in HKUST-1. The higher intensity reached by the $H_2\cdots Ni^{2+}$ complexes can be associated with the different natures of the adducts, as in this case an important charge transfer from the H_2 to the Ni is expected and then a higher polarization of the molecule. With respect to the interaction with the aromatic part of the MOFs, the highest intensities are also reached by CPO-27-Ni. A linear dependence of the intensities of the bands on the H−H frequency shift can be underlined, as it is visible in Figure 7.

However, by comparing the hydrogen amounts stored in these materials at 77 K and 45 bar, that is at low temperature and at high pressure as reported in the literature (1.8 for CPO-27-Ni,[16] 2.7 for HKUST-1, and 3.1 H_2 mass % for MOF-5),[3] we observe that the hydrogen capacities show an inverse dependence on $\Delta\tilde{\nu}$ (see Figure 8). In fact the lowest uptake is obtained for CPO-27-Ni, whereas the best performing material results in being the less reactive MOF-5. Actually this comparison is meaningful because, under these (P,T) conditions, e.g., in saturation condition, the stored amount mainly depends on the surface area and total pore volume of the material, showing almost no relationship with their activity.[3,56] This is visible in Figure 8, showing that the stored amounts have a linear and positive dependence on the surface area, as it has been reported previously for both low[57] and high pressure ranges.[58,59]

This means consequently that if control of MOF surface area can benefit the total stored amounts, only the presence of a great number of reactive sites can make the (P,T) storage conditions more economically favorable. In other words, the presence of coordinative unsaturated metal centers is crucial in determining the thermodynamic conditions of the first adsorbed H_2 molecules (temperature and ΔH_{ads}), while the quantitative amount of H_2 hosted at high pressures and low temperature reflects the available surface area of the materials. Summarizing, an improvement in the H_2 storage capability could be reached by synthesizing a new high surface area material hosting a very high surface density of metal centers.

Conclusions

The interaction of H_2 with three MOF materials has been studied by means of FTIR spectroscopy in the range 300 and 20 K. The MOFs taken in consideration have been chosen for the different natures and accessibilities of the metal sites present in their structure: MOF-5 (inaccessible metal sites), HKUST-1 (accessible Cu^{2+} sites), and CPO-27-Ni (accessible Ni^{2+} sites). Significantly different adsorption onset temperatures have been observed for the three materials: 180 K for CPO-27-Ni, 110 K for HKUST-1, and 105 K for MOF-5. These temperatures correlate with the enthalpy of adsorption obtained by means of the VTIR method[17,18] on these materials and with the shift experienced by the H−H stretching frequency after the adsorption. This relationship can be ascribed to the different natures and accessibilities of the metal sites. On the basis of a purely energetic evaluation, one may argue that the best performance is shown by CPO-27-Ni. However, by comparing the hydrogen amounts stored in these materials at high pressure (1.8 for CPO-27-Ni,[16] 2.7 for HKUST-1, and 3.1 H_2 mass % for MOF-5 at 77 K and 45 bar),[3] we observe that the hydrogen capacities in these conditions are mostly dependent on their surface area and total pore volume.[3] In fact, although a higher density of H_2 within the CPO-27-Ni pores than in the other two MOFs is expected because of the higher binding enthalpy,[60,61] this effect is almost completely hidden because of its significantly lower surface area and free volume.

However, if control of MOF surface area can benefit the total stored amounts, only the presence of a great number of reactive sites could allow milder (P,T) storage conditions. In particular, this seems to be one of the most important features to be taken into account in the "design" of new materials for H_2 storage. For example, concerning CPO-27-Ni, it can be predicted that if we consider one H_2 molecule adsorbed per Ni site at 180 K (a temperature only 10 K lower than that of dry ice) this material would be able to store about 1.27 mass % at pressures below 1 bar while only a negligible amount (less than 0.1 mass %) is expected for MOF-5 and HKUST-1 under the same (P,T) conditions. On the contrary, at higher pressures, all materials display adsorption capacities mostly correlated with the surface area. One route to better H_2 adsorbents is therefore the development of crystalline solids with a high surface density of adsorption sites.

Acknowledgment. The authors thank Jasmina Hafizovic (Oslo University) and Bo Xiao (St. Andrews University) for providing MOF-5 and HKUST-1 samples, respectively. Financial support by Regione Piemonte in the frame of the research project "Innovative materials for hydrogen storage" and by European VI framework through STREP project MOFCAT Contract No. NMP4-CT-2006-033335 are gratefully acknowledged.

(56) Panella, B.; Hirscher, M.; Putter, H.; Muller, U. *Adv. Funct. Mater.* **2006**, *16*, 520–524.
(57) Nijkamp, M. G.; Raaymakers, J. E. M. J.; van Dillen, A. J.; de Jong, K. P. *Appl. Phys. A* **2001**, *72*, 619–623.
(58) Panella, B.; Hirscher, M.; Roth, S. *Carbon* **2005**, *43*, 2209–2214.
(59) Poirier, E.; Chahine, R.; Bose, T. K. *Int. J. Hydrogen Energy* **2001**, *26*, 831–835.
(60) Frost, H.; Düren, T.; Snurr, R. Q. *J. Phys. Chem. B* **2006**, *110*, 9565–9570.
(61) Frost, H.; Snurr, R. Q. *J. Phys. Chem. C* **2007**, *111*, 18794–18803.

Supporting Information Available: Nitrogen adsorption/desorption isotherms at 77 K of the fresh and air-aged MOFs, table of the MOFs textural properties, description of the VTIR method, FTIR spectra of the as-prepared and dehydrated form of CPO-27-Ni, more detailed view of the first coordination sphere of the Ni ions in CPO-27-Ni, FTIR spectra of H_2 adsorbed on the MOFs including the rotovibrational region (registered upon lowering the temperature from 300 to 20 K), evolution of the FTIR spectra of H_2 adsorbed on the MOFs at 20 K upon degassing and list of the data reported in Figures 6–8. This material is available free of charge via the Internet at http://pubs.acs.org.

JA8007159